Electronic Supplementary Information

Experimental section

Materials: All reagents were directly utilized without further purification. $Co(NO_3)_2 \cdot 6H_2O$ (Shanghai Macklin Biochemical Co. Ltd), $CO(NH_2)_2$ (Shanghai Macklin Biochemical Co. Ltd), NH_4F (Sinopharm Chemical Reagent Co. Ltd), $NaH_2PO_2 \cdot H_2O$ (Shanghai Macklin Biochemical Co. Ltd), C_2H_5OH (Tianjin Fuyu Fine Chemical Co. Ltd), KOH (Sinopharm Chemical Reagent Co. Ltd), $NaBH_4$ (Chengdu Aikeda Chemical Reagent Co. Ltd), Carbon cloth (Ce Tech Co. Ltd), Platinum on carbon (20% Pt/C). The ultrapure water was purified through a Millipore system used throughout all experiments.

Synthesis of $Co(CO_3)_{0.5}(OH)_{0.11} \cdot H_2O$ nanorod array on CC (CoCH NRA/CC): Carbon cloth (CC) with area of 1 × 2 cm^2 was treated with nitric acid solution (34 wt%) at 60 °C for 2 h followed washing with ethanol and water, respectively. Treated CC was then dropped into Teflon-lined stainless reactors (20 ml) containing 16 ml ultrapure water, 0.72 mmol $Co(NO_3)_2 \cdot 6H_2O$, 1.8 mmol $CO(NH_2)_2$ and 0.72 mmol NH_4F. After the hydrothermal reaction conducting at 120 °C for 6h, CoCH NRA is generated on CC.

Fabrication of CoP NRA/CC: The obtained CoCH NRA/CC was put in the porcelain crucible, which was placed at the downstream end, while another porcelain crucible with 500 mg NaH_2PO_2 powder was placed at the upstream end of the furnace. The samples were annealing at 300 °C for 2 h under N_2 atmosphere to get CoP NRA/CC.

Synthesis of CoP-amorphous CoB hierarchical nanorod array (CoP@a-CoB HNRA) on CC: Firstly, CoP@$Co(OH)_2$ HNRA/CC was obtained by a chronoamperometry electrolysis strategy with the constant potential of -0.16 V (vs. RHE) for 8 h, which was performed in 1.0 M KOH by using the synthesized CoP NTA/CC as working electrode. Then the prepared CoP@$Co(OH)_2$ HNRA/CC was immersed in a mixed solution of 1.0 M $NaBH_4$ and 0.1 M NaOH for 1 min to obtain CoP@a-CoB HNRA. The CoP@a-CoB NRA without hierarchical structure was obtained through direct boronizing treatment of CoP NRA in 1.0 M $NaBH_4$ and 0.1 M NaOH for 1 min.

Synthesis of amorphous CoB nanosheet: In a typical procedure, 0.1 g $CoCl_2$ and 20 g $CO(NH_2)_2$ was blended and milled mechanically. The resultant pink mixture was transferred to a glass vessel. Then, the pink mixture was desiccated in an oven for about 15 min at 150 °C until the sample changed into blue in color. Subsequently, the milled

$NaBH_4$ powder was sprinkled on the mixture. After 48 h, the reaction is finished, only black products were observed. The obtained black powder was washed with ultrapure water, and finally desiccated in a vacuum oven at 60 ℃ for 6 h to obtain amorphous CoB nanosheet.

Characterizations: Powder X-ray diffraction (XRD) measurements were carried out on Rigaku Smartlab powder diffractometer using a Cu Ka radiation (λ= 1.5418 Å). Scanning electron microscope (SEM) images were obtained on JEOL JSM-7800F. Transition electron microscope (TEM), high-resolution TEM (HRTEM), high-angle annular dark field scanning TEM (HAADF-STEM) and elemental mappings were recorded on JEOL 2100F with 200 kV. The X-ray photoelectron spectroscopy (XPS) measurement was carried out on ESCALAB XI+ (Thermo Fisher), the binding energies were corrected by using C 1s peak of adventitious carbon to 284.5 eV.

Electrochemical measurements: All electrochemical tests were conducted with a standard three-electrode system on a CHI 760E station (CH instruments, China). The as-synthesized catalyst supported on CC was directly used as working electrode. As for contrastive Pt/C and a-CoB NS electrocatalysts, sample powder along with ethanol and Nafion were treated to form homogeneous solution. Then the well dispersed solution was dripped onto clean CC and naturally dried in air, finally generating the Pt/C and a-CoB mass loading of 0.1 mg cm^{-2} and 1.5 mg cm^{-2}, respectively. The graphite rod and saturated calomel electrode (SCE) serve as counter electrode and reference electrode, respectively. Linear sweep voltammetry (LSV) was tested to investigate the electrocatalytic activity in H_2-saturated 1.0 M KOH or 0.5 M H_2SO_4 at a scan rate of 10 mV s^{-1}. All the measured potentials were corrected with iR-compensation and referred to reversible hydrogen electrode (RHE) with the equation of E (vs RHE) = E (vs SCE) + 0.059*pH + 0.2415. Chronopotentiometry with the constant current density of 10 mA cm^{-2} and multi-current step test were used to evaluate the electrocatalytic stability. To estimate the electrochemical surface area (ECSA), the electrochemical double-layer capacitance (C_{dl}) measurements were carried out by using CVs with different scan rates of 20, 40, 60, 80, 100 mV s^{-1}. Electrochemical impedance spectroscopy (EIS) measurement were performed at the overpotentials of 72 mV and 59 mV in 1.0 M KOH and 0.5 M H_2SO_4, respectively, with frequency from 0.1 to 100 KHz.

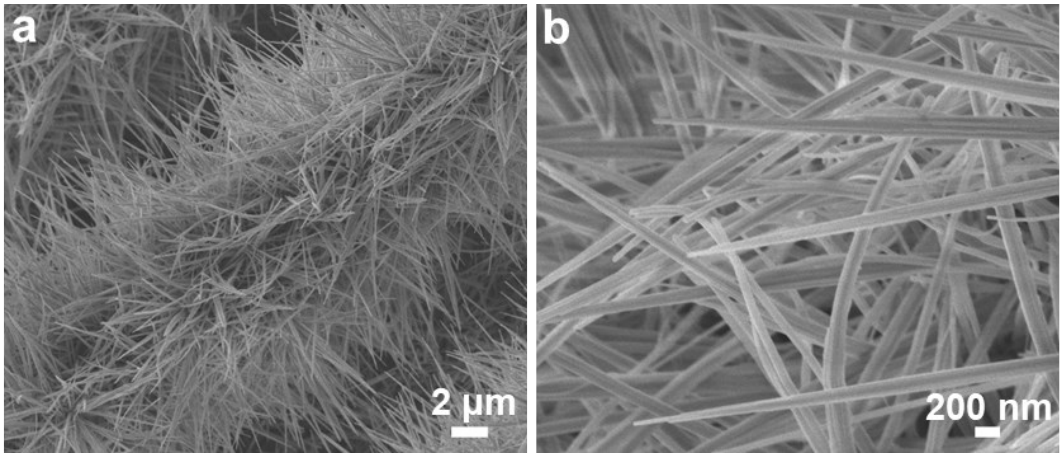

Fig. S1. SEM images of CoCH NRA on CC with low and high magnification.

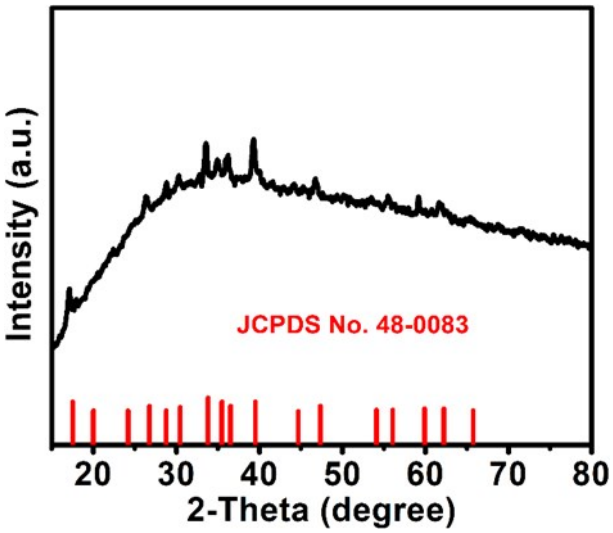

Fig. S2. XRD pattern of CoCH NRA.

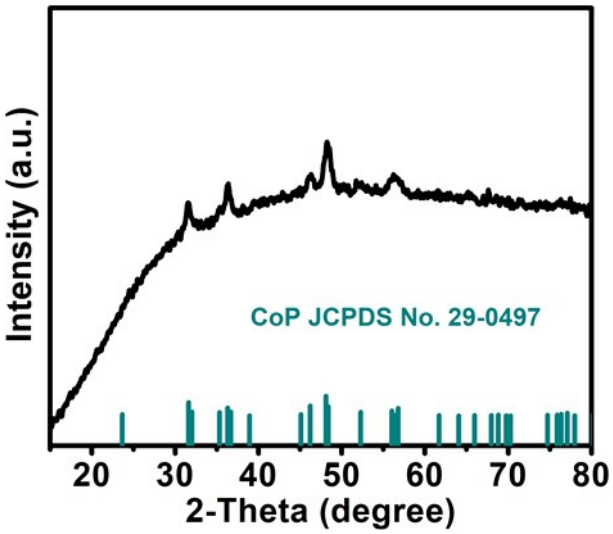

Fig. S3. XRD pattern of CoP NRA.

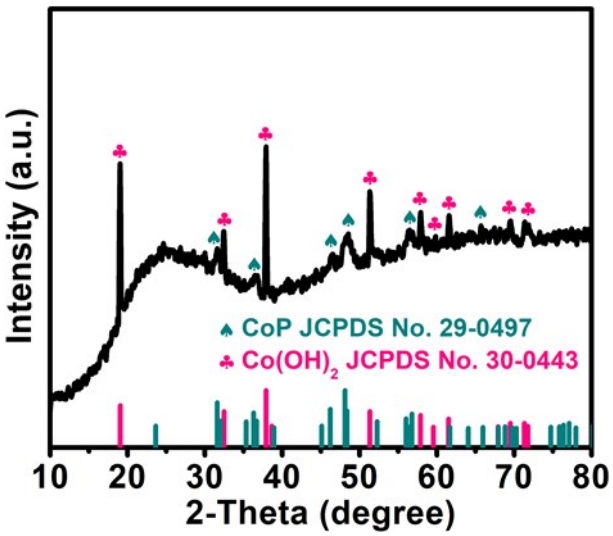

Fig. S4. XRD pattern of CoP@$Co(OH)_2$ HNRA.

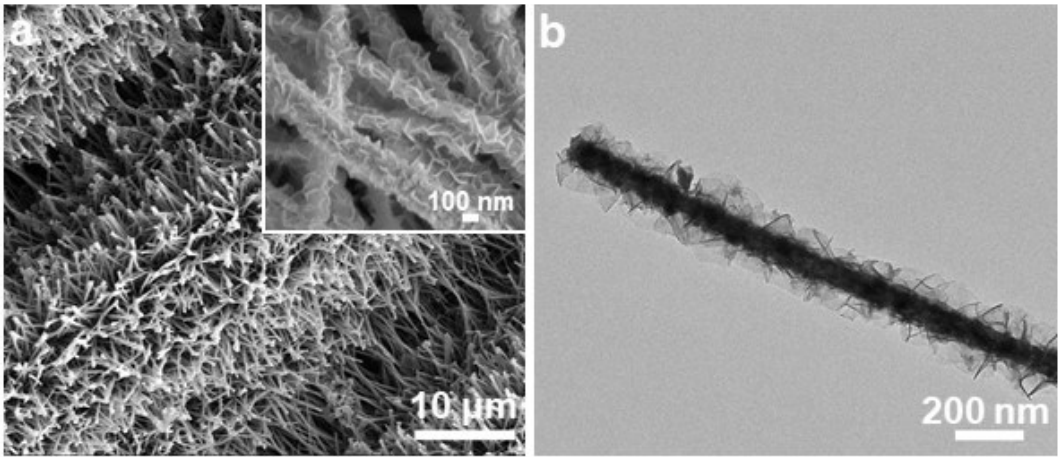

Fig. S5. (a) SEM images of CoP@$Co(OH)_2$ HNRA on CC with different magnification. (b) TEM image of single CoP@$Co(OH)_2$ hierarchical nanorod.

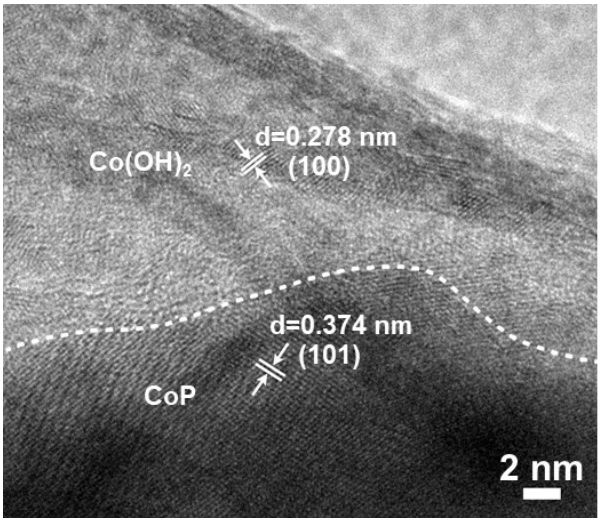

Fig. S6. HRTEM image of CoP@$Co(OH)_2$ HNRA.

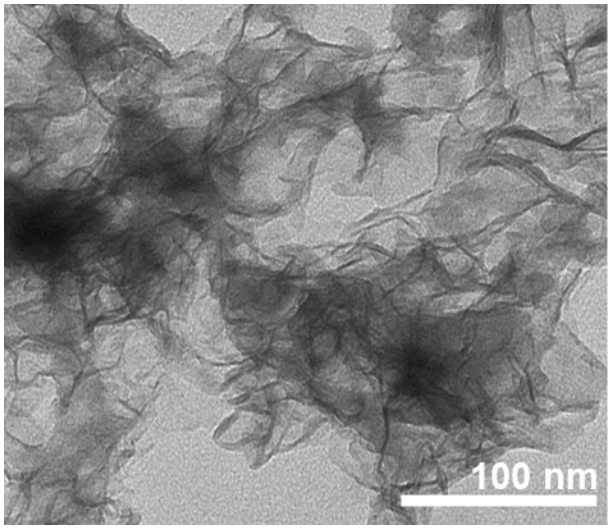

Fig. S7. TEM image of a-CoB NS.

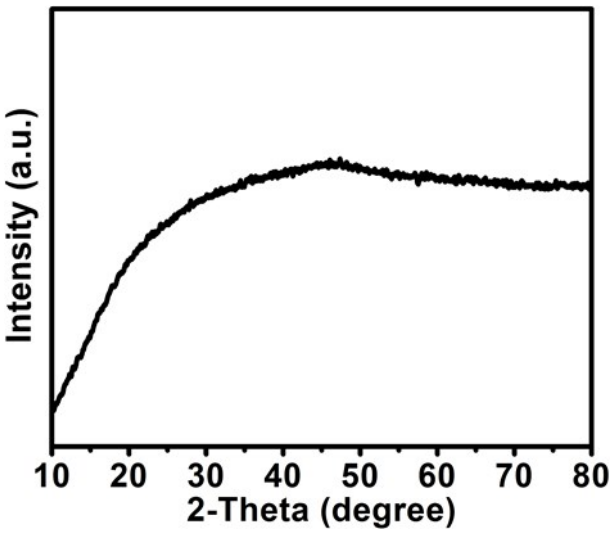

Fig. S8. XRD pattern of a-CoB NS.

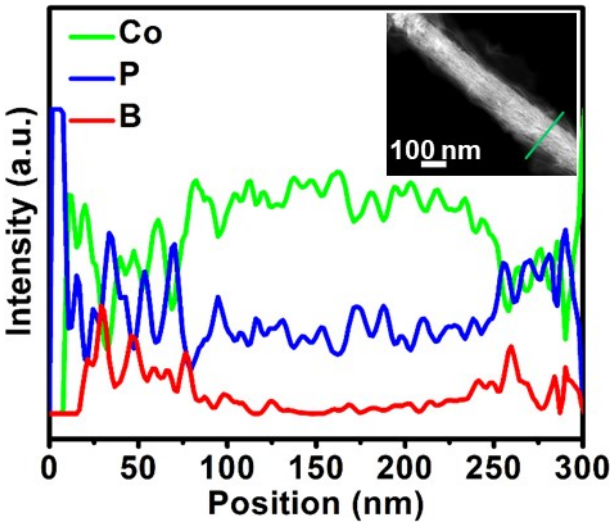

Fig. S9. The HAADF-STEM image of CoP@a-CoB hierarchical nanorod and corresponding line-scan profile.

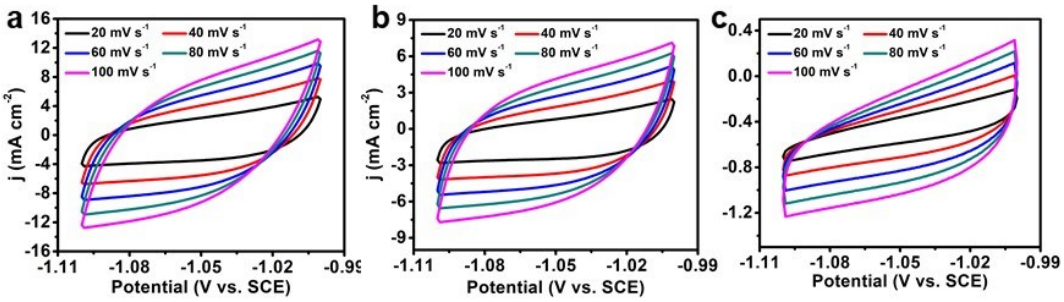

Fig. S10. CV curves of (a) CoP@a-CoB HNRA, (b) CoP NRA and (c) a-CoB NS with different scan rates (20-100 mV s^{-1}) in 1.0 M KOH.

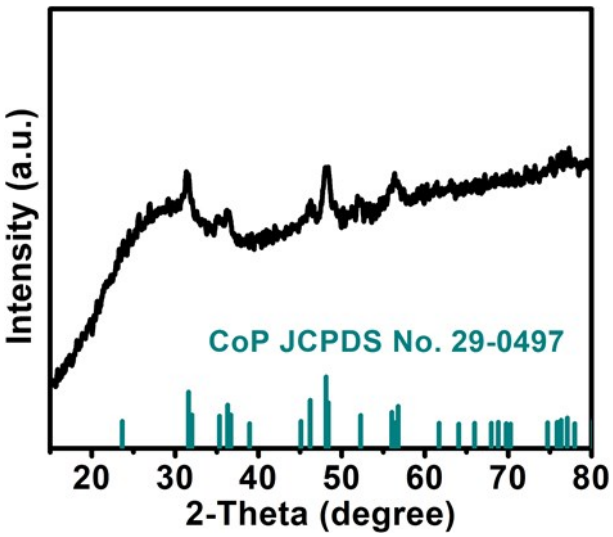

Fig. S11. XRD pattern of CoP@a-CoB NRA.

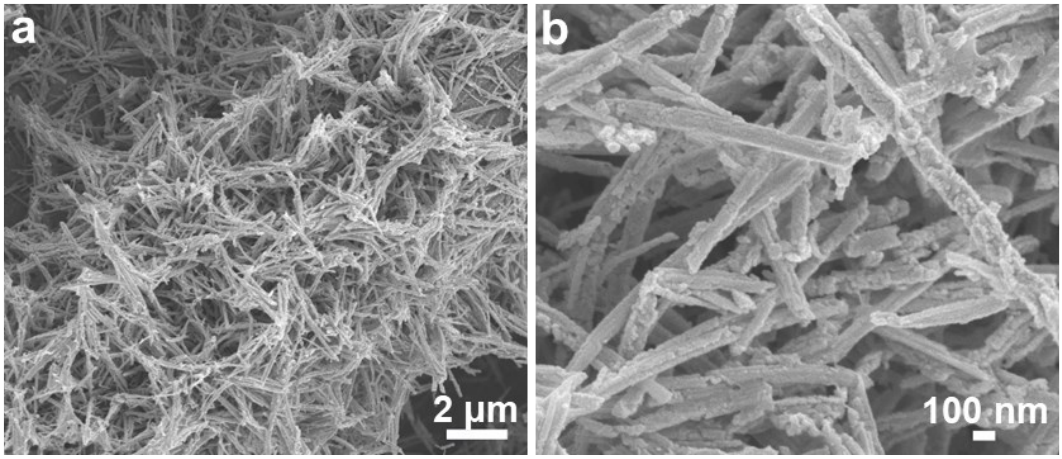

Fig. S12. SEM images of CoP@a-CoB NRA on CC with low and high magnification.

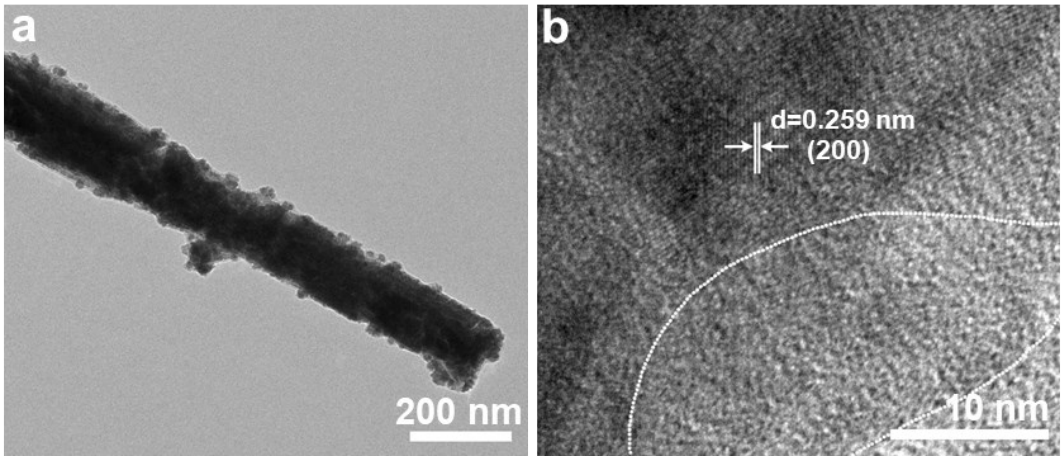

Fig. S13. (a) TEM image and (b) HRTEM image of CoP@a-CoB NRA.

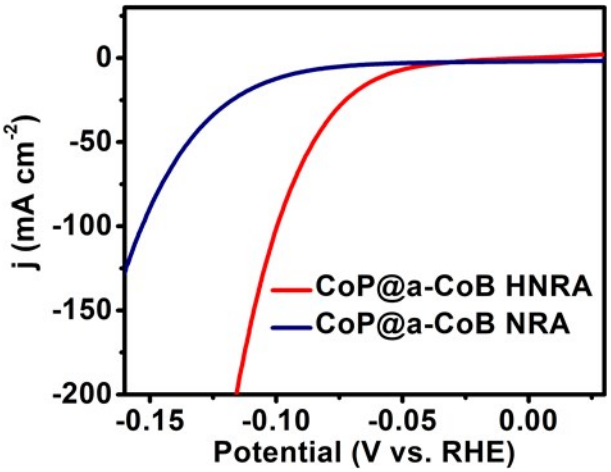

Fig. S14. Polarization curves of CoP@a-CoB HNRA and CoP@a-CoB NRA in 1.0 M KOH.

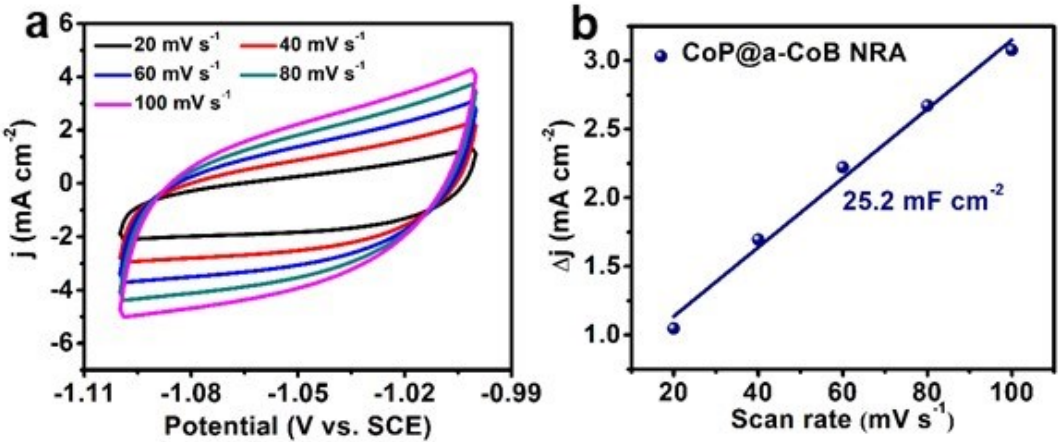

Fig. S15. (a) CV curves of CoP@a-CoB NRA with different scan rates (20-100 mV s^{-1}) in 1.0 M KOH. (b) The plot of capacitive current density as a function of scan rate at -1.05 V vs. SCE.

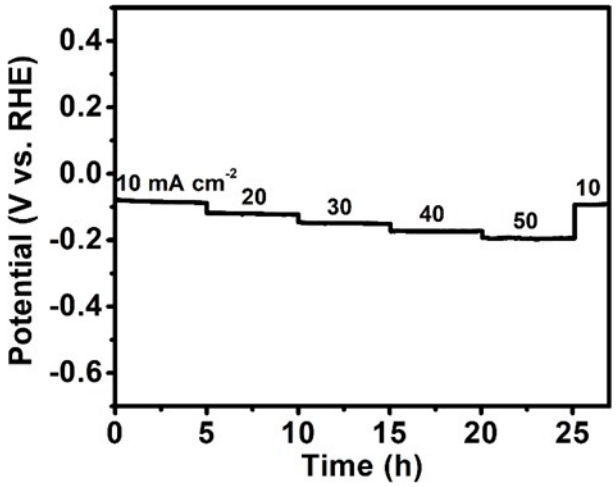

Fig. S16. Multi-current test at 10-50 mA cm^{-2} for CoP@a-CoB HNRA in 1.0 M KOH.

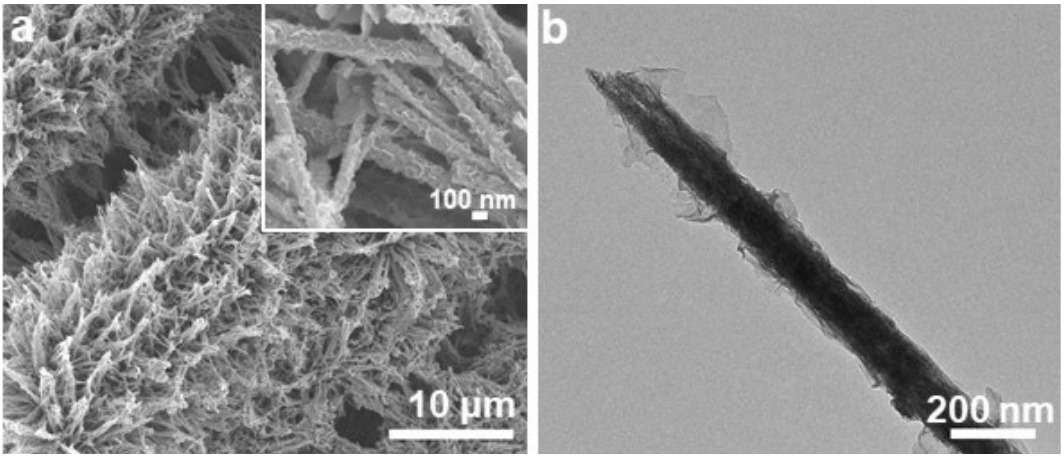

Fig. S17. The characterizations after stability test in 1.0 M KOH. (a) SEM images of CoP@a-CoB HNRA on CC and (b) TEM image of one CoP@a-CoB hierarchical nanorod.

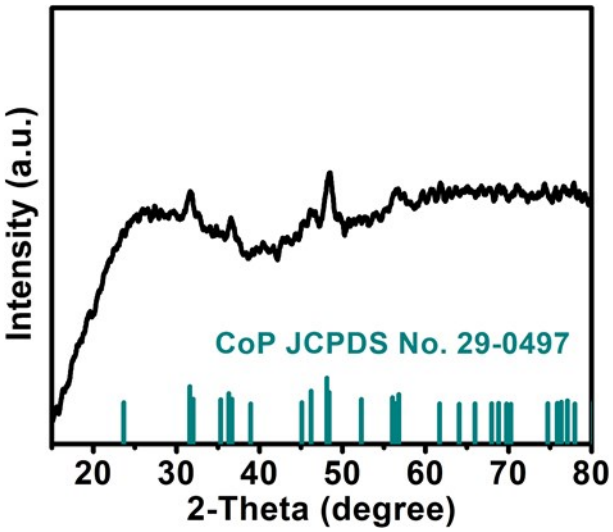

Fig. S18. XRD pattern of CoP@a-CoB HNRA after chronopotentiometry test in 1.0 M KOH.

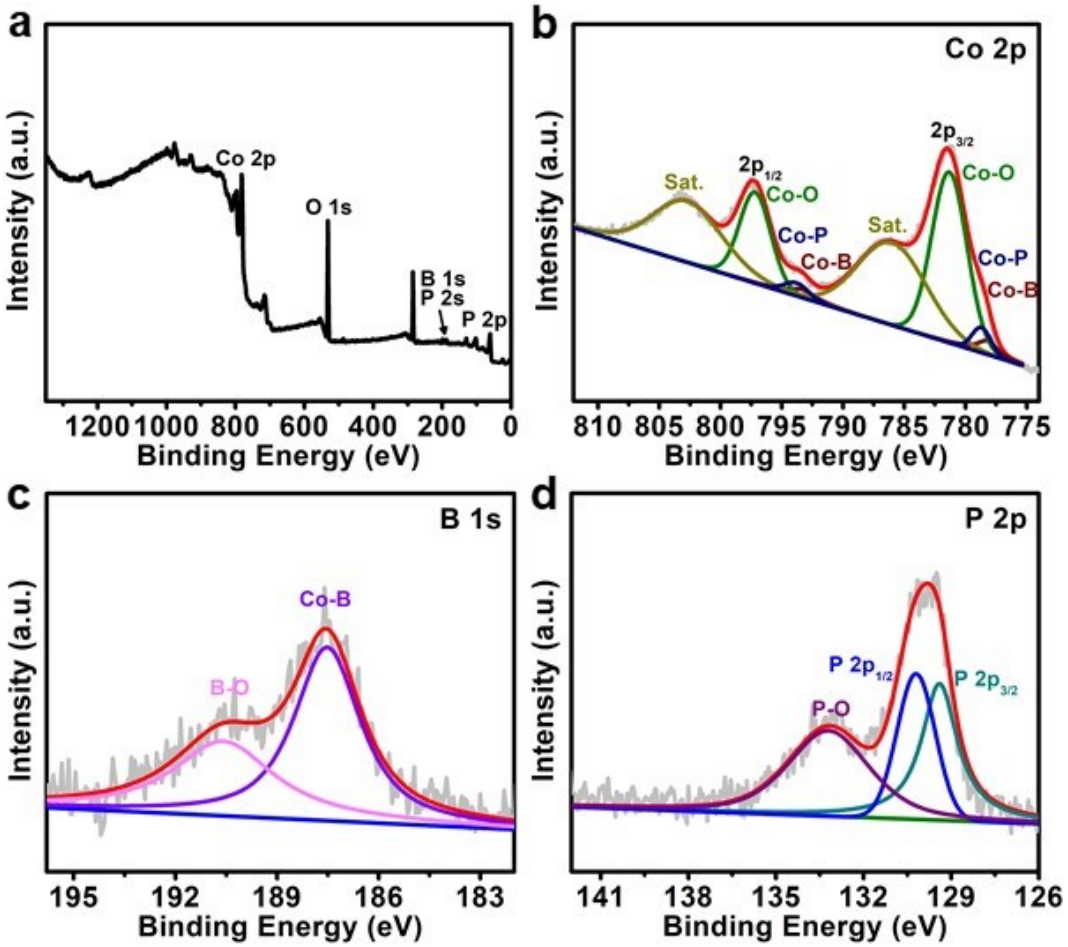

Fig. S19. The XPS characterizations of CoP@a-CoB HNRA after chronopotentiometry test in 1.0 M KOH. (a) Full XPS spectra. High-resolution XPS spectra of (b) Co 2p, (c) B 1s and (d) P 2p.

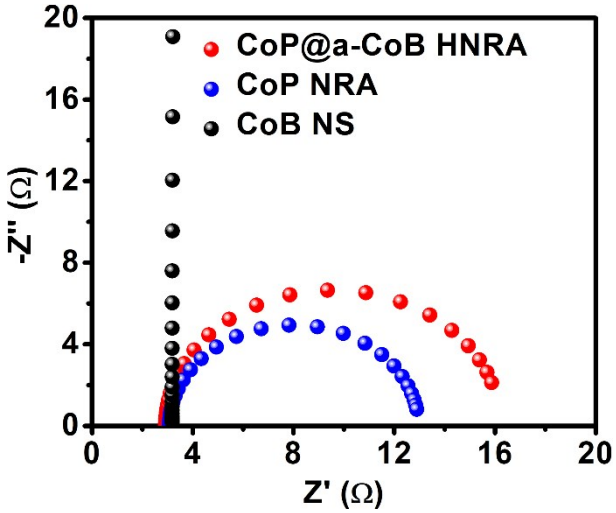

Fig. S20. EIS measurements of CoP@a-CoB HNRA, CoP NRA and CoB NS in 0.5 M H_2SO_4.

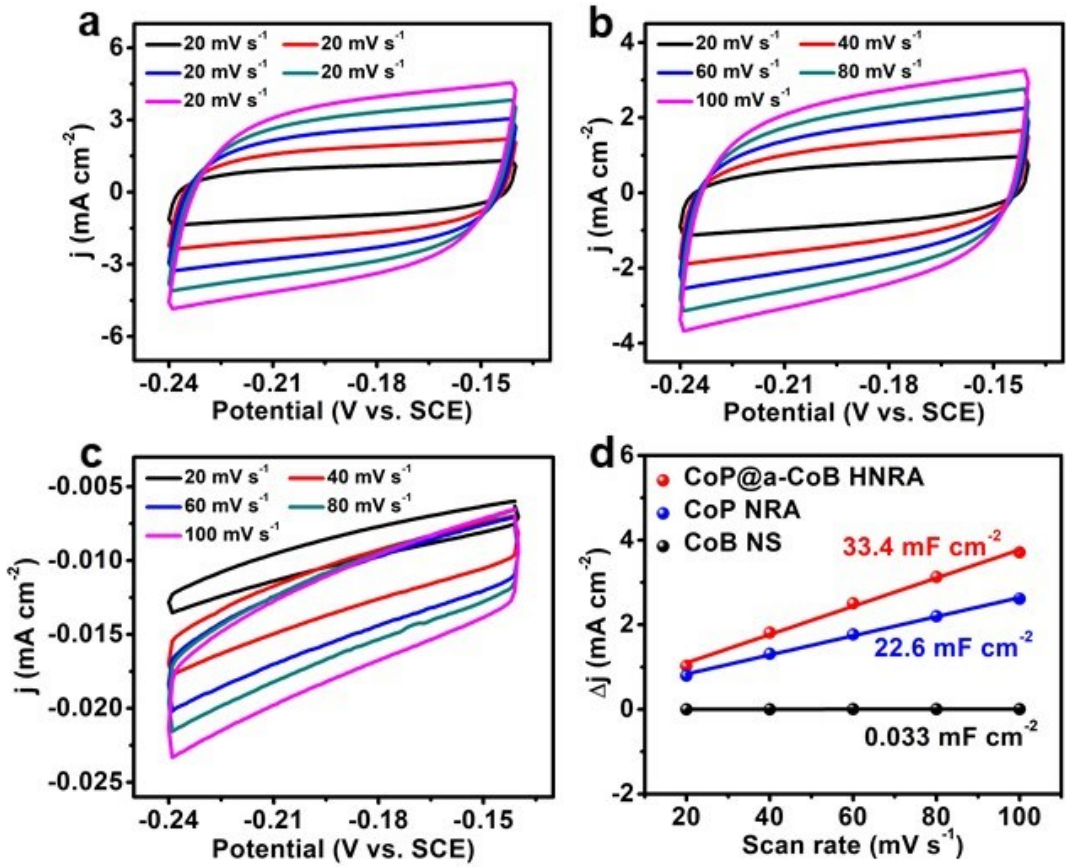

Fig. S21. CV curves of CoP@a-CoB HNRA (a), CoP NRA (b) and a-CoB NS (c) with different scan rates (20-100 mV s^{-1}) in 0.5 M H_2SO_4. (d) Plots of capacitive current density as a function of scan rate at -0.19 V vs. SCE.

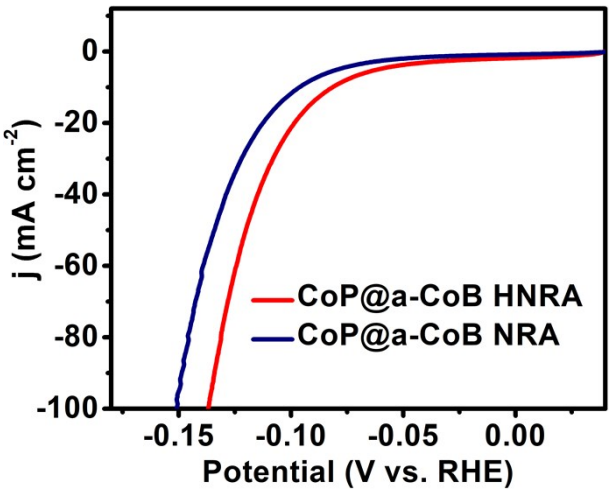

Fig. S22. Polarization curves of CoP@a-CoB HNRA and CoP@a-CoB NRA in 0.5 M H_2SO_4.

Table S1. The HER performance of CoP@a-CoB HNRA and reported electrocatalysts in alkaline solution.

Catalyst	Overpotential at 10 mA cm^{-2} (mV)	Tafel slope (mV dec^{-1})	Substrate	Electrolyte	Reference
CoP@a-CoB HNRA	**56.3**	**62.0**	**CC**	**1.0 M KOH**	**This work**
CoP/Ni_5P_4/CoP	71	58	NF	1.0 M KOH	1
Co/Co_2P@ACF/CNT	78	49	GCE	1.0 M KOH	2
NiCoFeB	345	98	GCE	1.0 M KOH	3
Co-Mo_2C-CNF	128	60	NFM	1.0 M KOH	4
N-CoP	39	58	CC	1.0 M KOH	5
$Ni_{0.89}Co_{0.11}Se_2$	85	52	NF	1.0 M KOH	6
N-Co-S/G	74.5	61.9	GCE	1.0 M KOH	7
Co_2P/CoNPC	208	83.9	GCE	1.0 M KOH	8
Ce-CoP	92	63.5	GCE	1.0 M KOH	9
C-Co_xP	121	62	GCE	1.0 M KOH	10
HNDCM-Co/CoP	135	64	PCM	1.0 M KOH	11
W-CoP	94	63	CC	1.0 M KOH	12

Table S2. The HER performance of CoP@a-CoB HNRAs and reported electrocatalysts in acidic solution.

Catalyst	Overpotential at 10 mA cm^{-2} (mV)	Tafel slope (mV dec^{-1})	Substrate	Electrolyte	Reference
CoP@a-CoB HNRA	81	55.4	**CC**	0.5 M H_2SO_4	This work
CoP–CNTs	139	58	GCE	0.5 M H_2SO_4	13
CoP	67	51	CC	0.5 M H_2SO_4	14
N-Co-S/G	67.7	56.3	GCE	0.5 M H_2SO_4	15
Ni_2P/OMM-CoN-C	68	37	GCE	0.5 M H_2SO_4	16
Ce-CoP	54	54	GCE	0.5 M H_2SO_4	9
C-Co_xP	109	55	GCE	0.5 M H_2SO_4	10
Co-P-B	172	68	CP	0.5 M H_2SO_4	17
HNDCM-Co/CoP	138	66	PCM	0.5 M H_2SO_4	18
$NiCo_2P_x$ nanowire	104	59.6	CF	0.5 M H_2SO_4	19
W-CoP NAs	89	58	CC	0.5 M H_2SO_4	12

References

1 I. K. Mishra, H. Zhou, J. Sun, F. Qin, K. Dahal, J. Bao, S. Chen and Z. Ren, *Energy Environ. Sci.*, 2018, **11**, 2246–2252.

2 F. Wang, L. Hu, R. Liu, H. Yang, T. Xiong, Y. Mao, M.-S. (J. Tang) Balogun, G. Ouyang and Y. Tong, *J. Mater. Chem. A*, 2019, **7**, 11150–11159.

3 Y. Li, B. Huang, Y. Sun, M. Luo, Y. Yang, Y. Qin, L. Wang, C. Li, F. Lv, W. Zhang and S. Guo, *Small*, 2019, **15**, 1804212.

4 J. Wang, R. Zhu, J. Cheng, Y. Song, M. Mao, F. Chen and Y. Cheng, *Chem. Eng. J.*, 2020, **379**, 125481.

5 Y. Men, P. Li, F. Yang, G. Cheng, S. Chen and W. Luo, *Appl. Catal. B*, 2019, **253**, 21–27.

6 B Liu, Y.-F. Zhao, H.-Q. Peng. Z.-Y. Zhang, C.-K. Sit, M.-F. Yuen, T.-R. Zhang and C.-S. Lee andW.-J. Zhang, *Adv. Mater.*, 2017, **29**, 1606521.

7 P. Sabhapathy, I. Shown, A. Sabbah, P. Raghunath, J.-L. Chen, W.-F. Chen, M.-C. Lin, K. H. Chen and L.-C. Chen, *Nano Energy*, 2021, **80**, 105544.

8 H. Liu, J. Guan, S. Yang, Y. Yu, R. Shao, Z. Zhang, M. Dou, F. Wang and Q. Xu, *Adv. Mater.,* 2020, **32**, 2003649.

9 W. Gao, M. Yan, H. Cheung, Z. Xia, X. Zhou, Y. Qin, C. Y. Wong, J. C. Ho, C. R. Chang and Y. Qu, *Nano Energy*, 2017, **38**, 290–296.

10 T.-S. Kim, H. J. Song, J.-C. Kim, B. Ju and D. W. Kim, *Small*, 2018, **14**, 1801284.

11 H. Wang, S. Min, Q. Wang, D. Li, G. Casillas, C. Ma, Y. Yang, Z. Liu, L.-J. Li, J. Yuan, M. Antonietti and T. Wu, *ACS Nano,* 2017, **11**, 4358–4364.

12 X. Wang, Y. Chen, B. Yu, Z. Wang, H. Wang, B. Sun, W. Li, D. Yang and W. Zhang, *Small,* 2019, **15**, 1902613.

13 C. Wu, Y. Yang, D. Dong, Y. Zhang and J. Li, *Small*, 2017, **13**, 1602873.

14 J. Tian, Q. Liu, A. M. Asiri and X. Sun, *J. Am. Chem. Soc.*, 2014, **136**, 7587–7590.

15 P. Sabhapathy, I. Shown, A. Sabbah, P. Raghunath, J.-L. Chen, W.-F. Chen, M.-C. Lin, K.-H. Chen and L.-C. Chen, *Nano Energy*, 2021, **80**, 105544.

16 T. Sun J. Dong, Y. Huang, W. Ran, J. Chen and L. Xu, *J. Mater. Chem. A*, 2018, **6**, 12751–12758.

17 J. Kim, H. Kim, S.-K. Kim and S. H. Ahn, *J. Mater. Chem. A,* 2018, 6, 6282–6288.

18 H. Wang, S. Min, Q. Wang, D. Li, G. Casillas, C. Ma, Y. Li, Z. Liu, L.-J. Li, J. Yuan, M. Antonietti and T. Wu, *ACS Nano,* 2017, **11**, 4358–4364.

19 R. Zhang, X. Wang, S. Yu, T. Wen, X. Zhu, F. Yang, X. Sun, X. Wang and W. Hu, *Adv. Mater.*, 2017, **29**, 1605502.